International Journal of Engineering

Journal Homepage: www.ije.ir

Characterization of Polypyrrole Hydroxyethyl Cellulose/TiO_2 Nanocomposite: Thermal Properties and AFM Analysis

M. Tanzifi*[a], Z. Taghipour Kolaei[b], M. Kolbadi nezhad[c], M. Roushani[d]

[a]*Department of Chemical Engineering, Faculty of Engineering, University of Ilam, Ilam, Iran*
[b]*Department of Chemical Engineering, Faculty of Engineering, Babol University of Technology, Babol, Iran*
[c]*School of Chemical Gas and Petroleum Engineering, Semnan University, Semnan, Iran*
[d]*Department of Chemistry, University of Ilam, Ilam, Iran*

PAPER INFO

Paper history:
Received 12 September 2014
Received in revised form 12 December 2014
Accepted 18 December 2014

Keywords:
Polypyrrole
Hydroxyethylcellulose
TitaniumDioxide
Thermal Properties
AFM Analysis

ABSTRACT

Polypyrrole hydroxyethyl cellulose/TitaniumDioxide (PPY-HEC/TiO_2) nanocomposite was synthesized via in situ chemical oxidative polymerization method at room temperature in water and water/ethyl acetate solution in the presence of ferric chloride ($FeCl_3$). The effect of TiO_2 nanoparticles and HEC on the characteristics of products such as thermal stability and morphology was investigated. The fabricated composite and nanocomposite morphology and structure were analyzed by atomic forced microscopy (AFM), Scanning electron microscope (SEM), Fourier transform infrared (FTIR) spectroscopy, X-ray diffraction (XRD) and Thermogravimetric analysis (TGA). The AFM images of products indicated that hydroxyethyl cellulose decreased the surface roughness of nanocomposite. Also, hydroxyethyl cellulose decreased particle size. The molecular structure of product was determined by FTIR spectroscopy. The results of XRD confirmed crystalline structure of TiO_2 nanoparticles and partly crystalline structure of PPY-HEC/TiO_2 nanocomposite. TGA was used to study the thermal behavior of nanocomposite. The TGA curves indicated that TiO_2 and HEC enhanced thermal stability of products.

***doi**: 10.5829/idosi.ije.2015.28.05b.02*

1. INTRODUCTION

Electrically conducting polymers like polyaniline (PAN), polypyrrole (PPY) and polythiophene (PTH) are of great interest as new class of materials in industry during the last two decades, owing to their unique combination of characteristics: electronic, optical, magnetic properties and processing advantage of polymers [1]. Synthesis of composites of conducting polymers with various materials has been reported. For instance, in some literatures [2-6], synthesized PAN/xanthan gum, PPY/xanthan gum, PAN/$CoFe_2O_4$, PAN/Sb_2O_3 and $CoFe_2O_4$/PAN/Ag nanocomposite, respectively. Polypyrrole can be prepared by electrochemical or chemical methods. Although the electrochemical polymerization of PPY leads to the formation of polymer thin film on working electrode, it is not suitable for mass production. Chemical oxidative polymerization is simple, cheap and fast [7].

TiO_2 is one of the main pigments which is usually used in the organic coatings [8] and nano-TiO_2 also has excellent physical and chemical properties, and it has been used in sensor, solar cell, photocatalyst, concrete and corrosion resistant film [9-14]. Polymer surfactants are important for a variety of industrial applications in the area of cosmetics, personal-care, food, pharmaceutics, detergents and mineral processing, and have drawn much attention in the last decades [15-19]. Compared with oligomer surfactants, polymer surfactants have many advantages such as densification, emulsification, decentralization, dissolution and film-building [19]. In 1980, a nonionic cellulose-based polymer surfactant was firstly patented by Landoll [20], which was synthesized by hydrophobically modified hydrotropic cellulose with long alkyl. Since then,

*Corresponding Author's Email: M.tanzifi@mail.ilam.ac.ir (M. Tanzifi)

Please cite this article as: M. Tanzifi, Z. Taghipour Kolaei, M. Kolbadi nezhad, M. Roushani,Characterization of Polypyrrole-hydroxyethylcellulose/TiO_2 nanocomposite: thermal properties and AFM analysis,International Journal of Engineering (IJE), TRANSACTIONS B: Applications Vol. 28, No. 5, (May 2015) 654-661

besides nonionic cellulose based polymer surfactants [21, 22], ionic [23], fluorocarbon [24] and amphoteric cellulose-based polymer surfactants [23, 25] have also been synthesized subsequently; they present many novel performances such as costless production, biodegradation and peculiar emulsification [26]. Hydroxyethyl cellulose (HEC), an important commercial water-soluble non-ionic polysaccharide, bears hydroxyl and ether proton-accepting groups and can form hydrogen bonds with proton-donors such as carboxylic acid groups. Because of its excellent biocompatibility and unique physicochemical properties, HEC has wide applications in the areas of coatings, fibers, dyeing, paper making, cosmetics, medicine, pesticides and oil exploitation [27, 28]. In this study, polypyrrole hydroxyethyl cellulose / TiO_2 nanocomposite was prepared in the aqueous and aqueous/non-aqueous solution using ferric chloride as an oxidant. Also products were investigated in terms of morphology, chemical structure and thermal stability.

2. EXPERIMENTAL

2. 1. Instrumentation The instruments used for this work included a magnetic stirrer (model HMS 8805, Iran), digital scale (model HP2 7HB, Sartorius, England), centrifuge (model Z-36HK), scanning electron microscope (SEM) (model KYKY-EM3200, China), Fourier-transform infrared (FTIR) spectrometer (model VERTEX 70; BRUKER, Germany), X-ray diffraction (XRD) (Philips model PW3040/60, Netherland), thermogravimetric analyzer (TGA) (PerkinElmer model 4000) and atomic force microscopy (AFM) (model Dualscope/Rasterscope C26, DME, Denmark). Also products were filtered on filter paper (model Whatman 41).

2. 2. Reagents and Standard Solutions Materials used in this work were pyrrole (d = 0.97 g/mL), hydroxyethyl cellulose (HEC) (M_W=4000, Figure 1) with an average number of substituted hydroxyl groups (DS) and a molar substitution degree (MS) of 1.5 and 2.5, respectively) from kalle-albert (Germany), ethyl acetate and ferric chloride, from Merck (Germany), and TiO_2 (rotile) from Kronos (Germany). All reagents were used as received without further purification, unless stated otherwise.

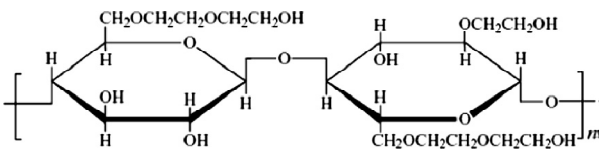

Figure 1. Chemical structure of HEC.

Distilled deionized water was used throughout this work. Pyrrole monomer was purified by simple distillation.

2.3. Polypyrrole Hydroxyethyl Cellulose / TiO_2 Nanocomposite In this method, 0.1 g hydroxyethyl cellulose was added to aqueous solution (50 ml water) and stirred for 3 h to dissolve. Then 0.1 g TiO_2 in nanometer size added to other stirred aqueous solution (50 ml water) containing 5.4 g $FeCl_3$. Then viscous solution of hydroxyethyl cellulose added to it. After 30 min, 1 ml pyrrole monomer was injected to the stirred solution.The reaction was carried out in aqueous media at room temperature for 5 h. After 5 h, the polymer was collected by centrifugation at 15000 rpm and in order to separate the oligomers and impurities, the product was washed several times with deionized water. It was then dried in a vacuum oven at 40 ^{0}C for 48 h. As a reference sample, pure PPY was prepared using same previous procedure without TiO_2 (solution of 100 ml containing 5.4 g $FeCl_3$ and 1 ml pyrrole monomer). Also the reaction was conducted in water/ethyl acetate solution at the room temperature for 5 h. The conditions for products formation are summarized in Table 1.

3. RESULTS AND DISCUSSION

3. 1. Atomic Force Microscopy Atomic force microscopy (AFM) was used to analyze the surface morphology and roughness of the products. The PPY/TiO_2 composite, pure HEC and PPY-HEC/TiO_2 nanocomposite surfaces were imaged in a scan size of 10 μm × 10 μm as shown in Figures 2-4. The surface roughness parameters of the materials which are expressed in terms of the mean roughness (Sa), the root mean square of the Z data (Sq) and the mean difference between the five highest peaks and lowest valleys (Sz) were calculated from AFM images using tapping mode method via Nanosurf EasyScan software at a scan area of 10 μm × 10 μm as given in Table 2.

TABLE 1. The conditions for products formation and their effect on the particle size.

Type of solution	Type of composite	Average particle size (nm)
Water	Pure Polypyrrole	140
Water	Polypyrrole + TiO_2	152
Water	Polypyrrole + HEC	98
Water	Polypyrrole + TiO_2 + HEC	102
Water + Ethyl Acetate (50/50% v/v)	Polypyrrole + HEC	68
Water + Ethyl Acetate (50/50% v/v)	Polypyrrole + TiO_2 + HEC	92

The film of pure HEC shows homogeneity, as it could be predicted. A different morphology with more roughness than that of HEC film is observed for a PPY/TiO_2 composite based film. As can be seen from the AFM image of synthesized nanocomposite (PPY-HEC/TiO_2) and reported parameters in Table 2, the surface roughness of nanocomposite is more than HEC and less than PPY/TiO_2 composite that it is probably due to the effect of HEC on the structure of PPY/TiO_2 composite.

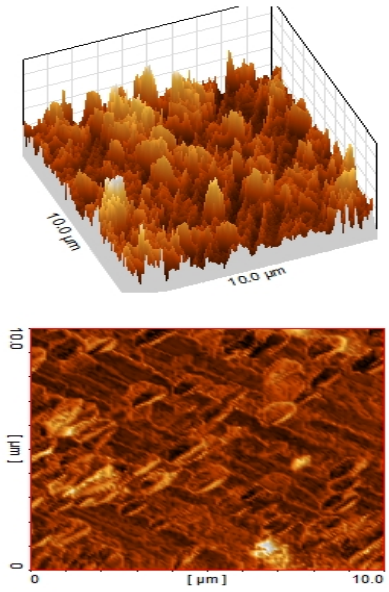

Figure 2. AFM images showing the 2D and 3D surfaces of PPY/TiO_2 composite (image size = 10mµ×10µm).

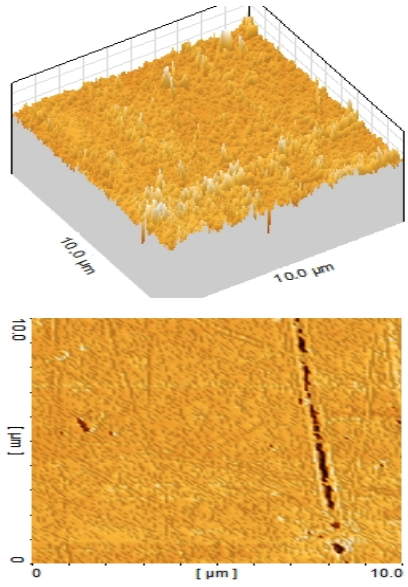

Figure 3. AFM images showing the 2D and 3D surfaces of pure HEC (image size = 10mµ×10µm).

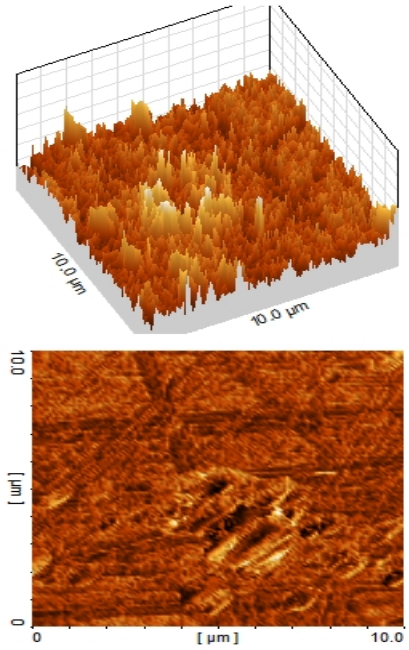

Figure 4. AFM images showing the 2D and 3D surfaces of PPY-HEC/TiO_2 nanocomposite (image size = 10mµ×10µm).

TABLE 2. Surface roughness parameters of pure HEC, PPY/TiO_2 and PPY-HEC/TiO_2 nanocomposite.

Sample	Roughness parameters		
	S_a	S_q	S_z
Pure HEC	8.22 nm	11.1 nm	73.1 nm
PPY/TiO_2	33.8 nm	44.9 nm	261 nm
PPY-HEC/TiO_2	16.1 nm	25.6 nm	110 nm

3. 2. SEM Analysis The morphology of composites and nanocomposites was studied using scanning electron micrographs (SEM). As shown in Figures 5 and 6, the role of HEC and TiO_2 on the surface morphology of the products was studied. Figure 5a shows the morphology of the TiO_2 nanoparticles. It indicates that nano-sized particles possess a nearly spherical morphology. The average diameter of TiO_2 nanoparticles is about 46 nm and its size distribution is highly uniform. Figures 5b-6d show the SEM micrographs of PPY and PPY/TiO_2 nanocomposite prepared in water and water/ethyl acetate with and without HEC. The particle size and morphology are dependent on the presence of TiO_2, HEC and type of solution. By comparison between Figures 5b and 6a , 6b, HEC strongly influenced the morphology of resultant product. Also, PPY-HEC/TiO_2 nanocomposite has the uniform size and smaller particles than PPY/TiO_2 (Figures 6c and 6d), because HEC prevented gross aggregation of particles. The size and homogeneity of particles are dependent on the

surfactant. This is presumably due to the amount of adsorbed chemically surfactant (grafting copolymer) on the polypyrrole particles. Surface active agents affect the physical and chemical properties of the solutions. Surfactant is known to influence the rate of polymer formation, particle size, size distribution, morphology and homogeneity [29-33].

It is clear to see that the PPY-TiO_2 composite (Figure 5c) with diameter of 152 nm tend to form bigger agglomerate. PPY-TiO_2 nanocomposite constructed in aqueous media using HEC has the uniform size with the average diameter of 102 nm (Figure 6c). The PPY/TiO_2 nanocomposite, prepared in aqueous/non-aqueous media using HEC, with highly uniform structure can be observed (Figure 6d). The average diameter of particles was less than 92 nm.

It was found that in the preparation of PPY and PPY/TiO_2 nanocomposite in water+ethyl acetate solution, polydispersity increased, particle size decreased, and spherical/granular particles were formed, because the physical and chemical properties of the solution affected the rate of polymerization. Particle size of products is listed in Table 1. As shown in this table, particle size of PPY and PPY-HEC without TiO_2 is less than PPY/TiO_2 and PPY-HEC/TiO_2 nanocomposite, respectively. It can be seen that the TiO_2 nanoparticles are surrounded by amorphous organice PPY. The average particle size of products was measured by measurement software. About 30-35 particles was chosen and average particle size was calculated.

3. 3. Fourier Transfer Infrared Spectroscopy

The structure of obtained products was determined by the FTIR spectrum. Figures 7 and 8, show the FTIR spectra of pure PPY, pure HEC, PPY-HEC, PPY/TiO_2 and PPY HEC/TiO_2, respectively. The FTIR spectroscopy provides valuable information regarding the formation of PPY composites and nanocomposites.

For pure PPY sample (Figure 7a), the peak at 1530 cm^{-1} is assigned to the pyrrole rings. The other peaks are located at 1286 cm^{-1} (C-N stretching vibration), 1147 cm^{-1} (C-H inplane deformation), 1027 cm^{-1} (N-H in-plane deformation), and 884 cm^{-1} (C-H out-of-plane deformation). In the spectrum of pure HEC (Figure 7b), the absorption bands around 3434, 2898 and 1054 cm^{-1} correspond to the O-H of alcoholic hydroxyl groups, C-H aliphatic stretching vibrations and C–O of primary hydroxyl groups, respectively.

The FTIR spectra of nanocomposites reveal that all of the characteristic peaks of both HEC and PPY exist in the synthesized nanocomposites structure as shown in Figure 7 and 8. For example the PPY-HEC/TiO_2 nanocomposite has the characteristic bands at 3635, 2998, 1534, 1289, 1160, 1058, 1030 and 887 cm^{-1} which are attributed to O-H band of HEC, C-H band of HEC, pyrrole rings, C-N band of PPY, C-H band of PPY, C-O band of HEC, N-H group of PPY and C-H band of PPY, respectively. The observed peaks of pure HEC, pure PPY and its composites are given in Table 3.

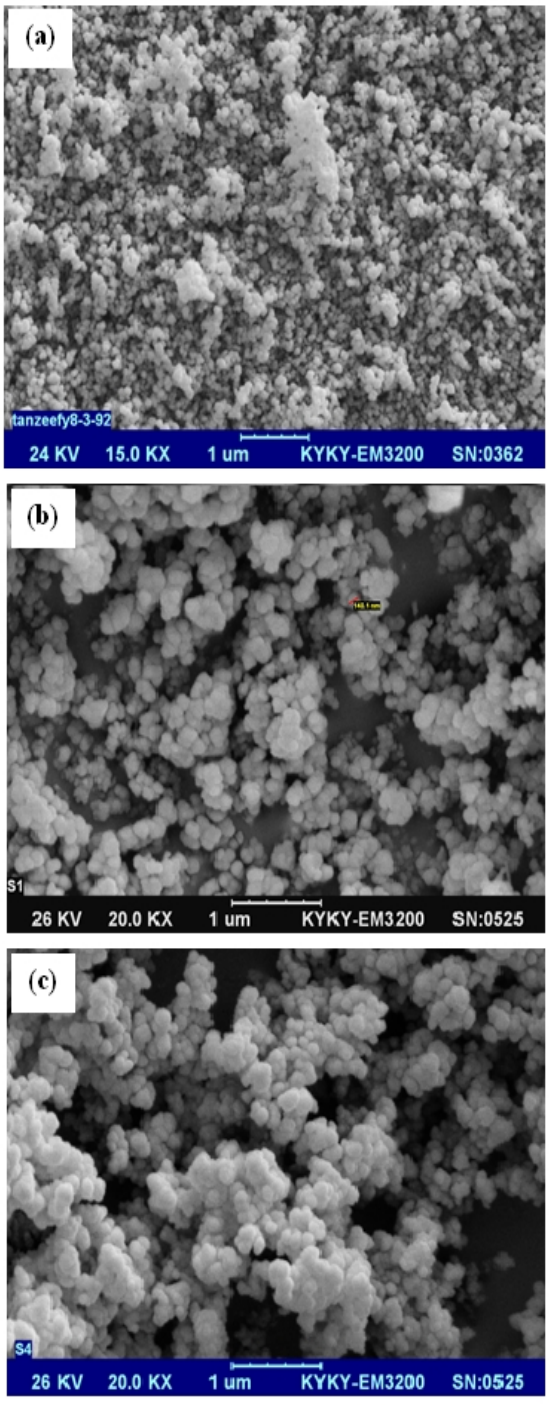

Figure 5. SEM micrographs of (a) pure TiO_2, (b) pure PPY and (c) PPY/TiO_2 composite

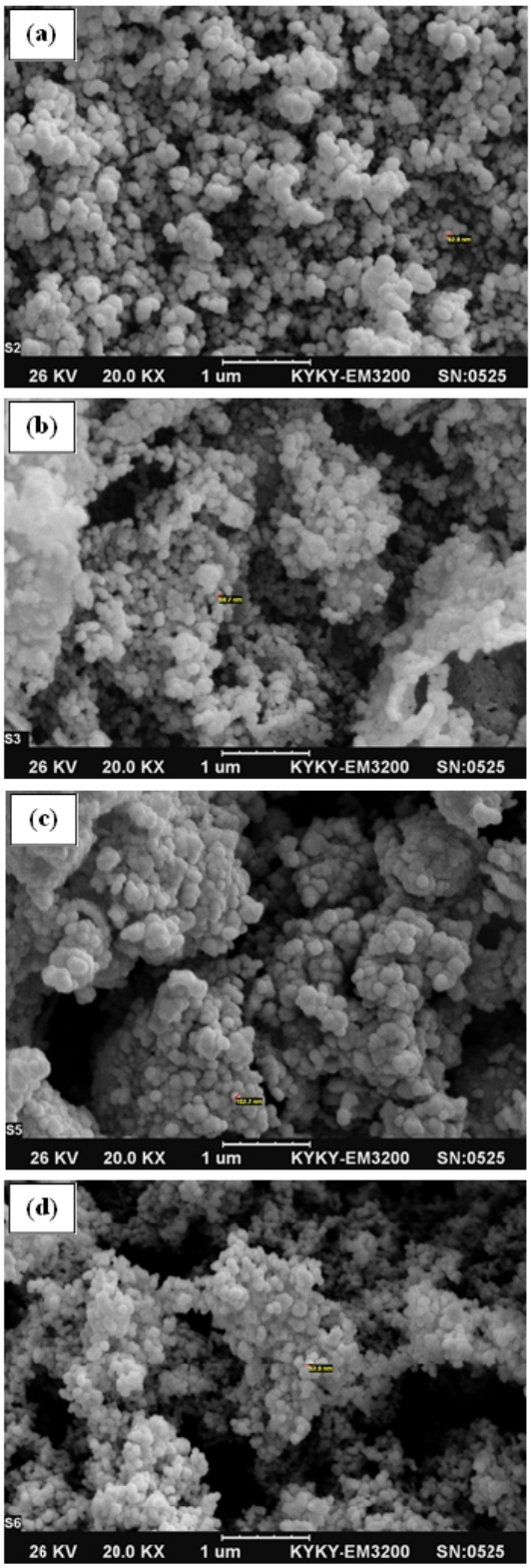

Figure 6. SEM micrographs of (a) PPY-HEC in aqueous media, (b) PPY-HEC in aqueous/non-aqueous media, (c) PPY-HEC/TiO_2 nanocomposite in aqueous media and (d) PPY-HEC/TiO_2 nanocomposite in aqueous/non-aqueous media.

TABLE 3. FTIR spectra of pure PPY and its composite and nanocomposite.

	FTIR Spectra			FTIR Composite	
	HEC	**PPY**	**PPY-TiO_2**	**PPY-HEC**	**PPY-HEC/TiO_2**
O-H[a]	3434	-	-	3675	3635
C-H[b]	2898	-	-	3006	2998
C-O[c]	1054	-	-	1062	1058
C=C[d]	-	1530	1522	1519	1534
C-N[e]	-	1286	1281	1282	1289
C-H[f]	-	1147	1128	1127	1160
N-H[g]	-	1027	1008	1005	1030
C-H[h]	-	884	834	841	887

[a] O-H alcoholic hydroxyl groups
[b] C-H aliphatic stretching vibrations
[c] C-O primary hydroxyl groups
[d] C=C stretching
[e] C-N stretching vibration
[f] C-H in-plane deformation
[g] N-H in-plane deformation
[h] C-H out of plane deformation

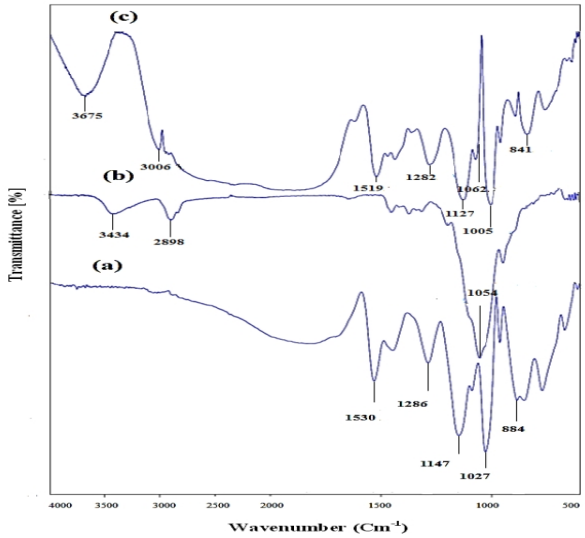

Figure 7. FTIR spectra of (a) pure PPY, (b) pure HEC and (c) PPY-HEC nanocomposite in aqueous media.

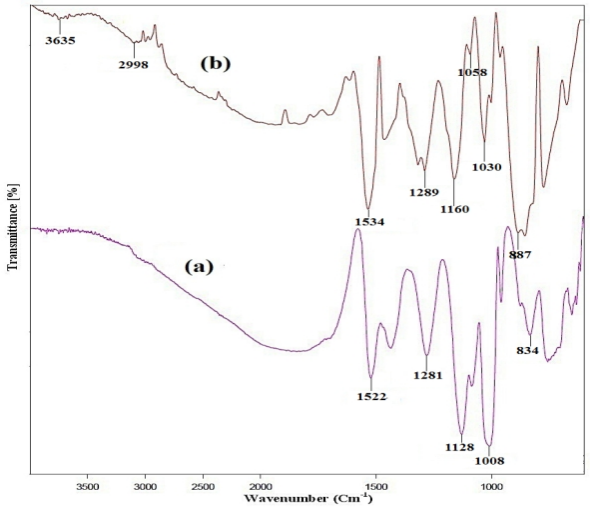

Figure 8. FTIR spectra of (a) PPY/TiO_2 and (b) PPY-HEC/TiO_2 nanocomposite in aqueous media.

3. 4. X-ray Powder Diffraction The crystalline nature of the nanocomposite was determined from XRD analysis. XRD patterns of pure PPY, pure TiO_2 and PPY-HEC/TiO_2 nanocomposite are shown in Figure 9. PPY is innately amorphous and therefore, there are no sharp peaks for PPY (Figure 9a). As can be seen in Figure 9c, XRD pattern of PPY-HEC/TiO_2 nanocomposite exhibit a predominant TiO_2 peaks than PPY. The broad peak with 2θ around 25.4° is related to the diffraction of amorphous polypyrrole and other peaks with 2θ at 27°, 39.2° and 55.1° are related to diffraction of TiO_2, respectively.

The average crystallite size was estimated from the intensity of the X-ray diffraction peak maximum using the Scherrer's equation, $L=k\lambda/\beta\cos\theta$, where L is the mean dimension of the crystallite, β is the full width at half maximum of the diffraction peak, θ is the diffraction angle, λ is the X-ray wavelength and K is the shape factor and if the shape is unknown, k is often assigned a value of 0.89 [34].

When the reflecting peak at 2θ = 27° is chosen for calculating the average diameter, the average size of the crystals of pure TiO_2 and PPY-HEC/TiO_2 core-shell nanocomposite is achieved as 45 and 100 nm which is consistent with the result of the SEM. Calculated crystallite sizes of pure TiO_2 nanoparticles and PPY-HEC/TiO_2 core-shell nanocomposite indicate that the thickness of PPY-HEC shell on the surface of TiO_2 nanoparticles in PPY-HEC/TiO_2 core-shell nanocomposite is ~50 nm.

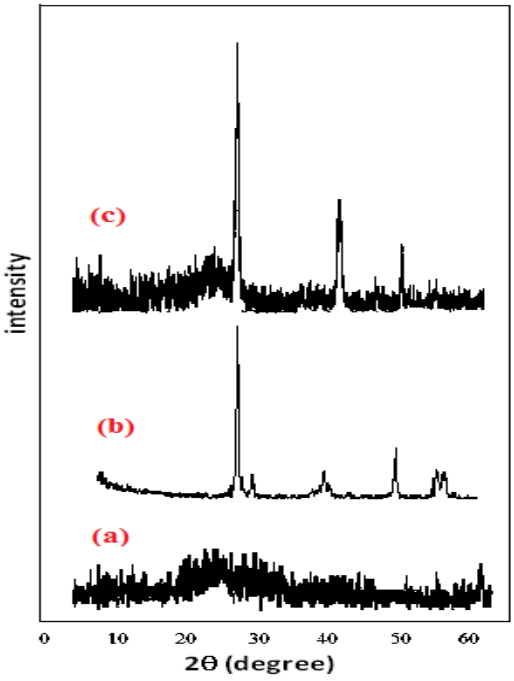

Figure 9. XRD pattern of (a) pure PPY, (b) TiO_2 and (c) PPY-HEC/TiO_2 nanocomposites in aqueous/non-aqueous media.

3. 5. Thermogravimetric Analysis In order to understand the effect of HEC and TiO_2 on the thermal stability of Polypyrrole and its composites, TGA analysis was used to identify the thermal stability of these composites.

Figure 10 shows a comparison of the weight losses between the PPY, PPY/TiO_2 and PPY-HEC/TiO_2 nanocomposites, upon heating in a nitrogen atmosphere with the temperature range of 25–600 °C at a rate of 10 °C min^{-1}. Three steps of weight loss occurred in the TGA curve of PPY samples. The thermogram of pure polypyrrole (Figure 10a) shows that the mass loss begins at around 30°C and continues until temperature reaches to 140°C. The mass loss remains steady until 320 °C and then a rapid mass loss occurred from 320 °C to 600 °C. At first, the mass loss comes from the loss of water molecules and then it is increased due to the loss of oligomer. The subsequent rapid mass loss can be attributed to the degradation of the polymer chain.

As shown in TGA plot (Figure 10b), the expulsion of water molecules retained in the polymer matrix which can be assigned to the adsorbed water due to the mesoporous structure of as-prepared samples [35], causes the first step weight loss for the PPY/TiO_2 composite (about 7 wt.% from 27°C to 148°C). There are two possible reasons for the second wight loss occurring between 148 and 380°C: (i) the loss of more tightly bound water in the matrix for the composites and (ii) the loss of volatile elements bound to the PPY chain as well as the elimination of interaction between PPY and TiO_2. The following progressive degradation and combustion of PPY, can be the driving force for the weight loss in the temperature range of ~400–600 °C. The weight loss between 200°C and 380°C (Figure 10c) could be attributed to the evaporation and degradation of HEC.

In addition, it has been found that the extent of thermal decomposition of PPY in nanocomposites, at temperatures higher than ~ 350°C, becomes lower than pure PPY. As can be seen in Figure 10, it was found that the weight loss of pure PPY is ~ 30% higher than the PPY/TiO_2 composite and 62% higher than the PPY-HEC/TiO_2 nanocomposite.

4. CONCLUSION

In this paper, Polypyrrole-hydroxyethyl cellulose /TiO_2 nanocomposite was synthesized via in situ chemical oxidative polymerization method at room temperature in aqueous and aqueous/non-aqueous media. The characteristics of PPY–HEC/TiO_2 nanocomposite, such as morphology, molecular structure and thermal stability were investigated. It was found that the TiO_2 nanoparticles and HEC have an important effect on the particle size and morphology of the resulting products.

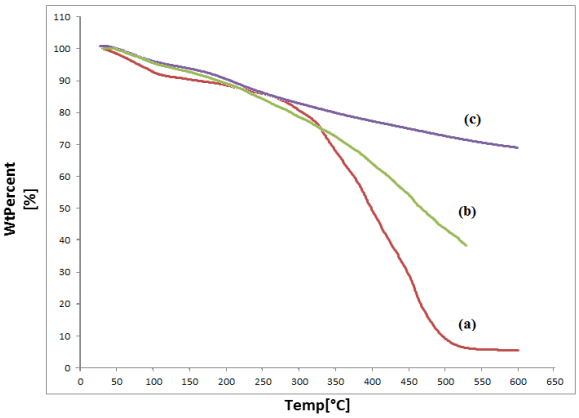

Figure 10. TGA curves of (a) pure PPY, (b) PPY/TiO_2 composite and (c) PPY-HEC/TiO_2 nanocomposite.

The AFM images of products indicate that hydroxyethyl cellulose decreased the surface roughness of nanocomposite. The results show that the surface roughness of PPY-HEC/TiO_2 nanocomposite is more than HEC and less than PPY/TiO_2 composite that it is due to the effect of HEC on the structure of PPY/TiO_2 composite. The chemical structure of synthesized nanocomposites was analyzed by FTIR. The results of XRD demonstrate the crystalline structure of TiO_2 nanoparticles and partly crystalline structure of PPY-HEC/TiO_2 nanocomposite. Using Scherrer's equation, the average size of the pure TiO_2 and PPY-HEC/TiO_2 nanocomposite was achieved as 45 and 100 nm which is consistent with the result of the SEM.

Thermal degradation behavior of products was compared and results show that thermal stability of PPY/TiO_2 is better than pure PPY. Also, thermal stability of PPY-HEC/TiO_2 nanocomposite is better than both of them.

5. REFERENCES

1. Shaktawat, V., Sharma, K. and Saxena, N., "Structural and electrical characterization of protonic acid doped polypyrrole", ***Journal of Ovonic Research***, Vol. 6, (2010), 239-245.
2. Larimi, S.G., Darzi, H. H. and Darzi, G.N., "Fabrication and characterization of polyaniline/xanthan gum nanocomposite: Conductivity and thermal properties", ***Synthetic Metals***, Vol. 162, No. 1, (2012), 171-175.
3. Darzi, H. H., Larimi, S.G. and Darzi, G.N., "Synthesis, characterization and physical properties of a novel xanthan gum/polypyrrole nanocomposite", ***Synthetic Metals***, Vol. 162, No. 1, (2012), 236-239.
4. Vaezi, M., Nikzad, L. and Yazdani, B., "Synthesis of cofe 2o4-polyaniline nanocomposite and evaluation of its magnetic properties", (2009).
5. Khalili, R. and Eisazadeh, H., "Preparation and characterization of polyaniline/sb2o3 nanocomposite and its application for removal of pb (ii) from aqueous media", ***International Journal of Engineering-Transactions B: Applications***, Vol. 27, No. 2, (2013), 239-346.
6. Kooti, M., Kharazi, P. and Motamedi, H., "Preparation, characterization, and antibacterial activity of cofe 2 o 4/polyaniline/ag nanocomposite", ***Journal of the Taiwan Institute of Chemical Engineers***, Vol. 45, No. 5, (2014), 2698-2704.
7. Zhang, X., Zhang, J., Wang, R., Zhu, T. and Liu, Z., "Surfactant-directed polypyrrole/cnt nanocables: Synthesis, characterization, and enhanced electrical properties", ***Chemical Physics and Physical Chemistery,*** Vol. 5, No. 7, (2004), 998-1002.
8. Sathiyanarayanan, S., Azim, S.S. and Venkatachari, G., "Preparation of polyaniline–tio 2 composite and its comparative corrosion protection performance with polyaniline", ***Synthetic Metals***, Vol. 157, No. 4, (2007), 205-213.
9. Zhou, W., Sun, C.-W. and Yang, Z.-Z., "Research and development of titania oxygen sensors", ***Journal of Inorganic Materials***, Vol. 13, No. 3, (1998), 275-281.
10. Boroumandnia, A., Kasaeian, A., Nikfarjam, A. and Mohammadpour, R., "Effect of tio2 nanofiber density on organic-inorganic based hybrid solar cells", ***International Journal of Engineering***, Vol. 27, No. 7, (2014) 345-356.
11. Machida, M., Norimoto, K., Watanabe, T.e., Hashimoto, K. and Fujishima, A., "The effect of sio2 addition in super-hydrophilic property of tio2 photocatalyst", ***Journal of Materials science***, Vol. 34, No. 11, (1999), 2569-2574.
12. Nazari, A. and Riahi, S., "Tio 2 nanoparticles effects on physical, thermal and mechanical properties of self compacting concrete with ground granulated blast furnace slag as binder", ***Energy and Buildings***, Vol. 43, No. 4, (2011), 995-1002.
13. Jalal, M., Ramezanianpour, A.A. and Pool, M.K., "Split tensile strength of binary blended self compacting concrete containing low volume fly ash and tio 2 nanoparticles", ***Composites Part B: Engineering***, Vol. 55, (2013), 324-337.
14. Khalili, V., Khalil-Allafi, J. and Maleki-Ghaleh, H., "Titanium oxide (tio2) coatings on niti shape memory substrate using electrophoretic deposition process", ***International Journal of Engineering***, Vol. 26, (2013), 707-712.
15. Zana, R., "Micellization of amphiphiles: Selected aspects", ***Colloids and Surfaces A: Physicochemical and Engineering Aspects***, Vol. 123, (1997), 27-35.
16. Zaitsev, S.Y., Generalova, A., Marchenko, S., Makievski, A., Krägel, J. and Miller, R., "Influence of polymeric non-ionic surfactants on the surface tension of styrene and on the styrene polymerization process", ***Colloids and Surfaces A: Physicochemical and Engineering Aspects***, Vol. 239, No. 1, (2004), 145-149.
17. Audibert-Hayet, A. and Dalmazzone, C., "Surfactant system for water-based well fluids", ***Colloids and Surfaces A: Physicochemical and Engineering Aspects***, Vol. 288, No. 1, (2006), 113-120.
18. Chuev, G.N. and Fedorov, M.V., "Density functional study of fluorocarbon emulsions with adsorbed polymer surfactant", ***Journal of molecular liquids***, Vol. 120, No. 1, (2005), 155-157.
19. Shen, Y., "Polymeric surfactants", ***Chemical Industry Press, Beijing***, (2002).
20. Landoll, L.M., *Modified nonionic cellulose ethers.* Google Patents. (1980),
21. Um, S.-U., Poptoshev, E. and Pugh, R., "Aqueous solutions of ethyl (hydroxyethyl) cellulose and hydrophobic modified ethyl (hydroxyethyl) cellulose polymer: Dynamic surface tension measurements", ***Journal of Colloid and Interface Science***, Vol. 193, No. 1, (1997), 41-49.
22. Evani, S., *Water soluble polymer, surfactant, and salt-used in enhanced oil recovery.* 1984, Google Patents.

23. Li, Z., Wang, L. and Huang, Y., "Photoinduced graft copolymerization of polymer surfactants based on hydroxyethyl cellulose", ***Journal of Photochemistry and Photobiology A: Chemistry***, Vol. 190, No. 1, (2007), 9-14.
24. Hwang, F. and Hogen-Esch, T., "Fluorocarbon-modified water-soluble cellulose derivatives", ***Macromolecules***, Vol. 26, No. 12, (1993), 3156-3160.
25. Cao, Y. and Li, H., "Interfacial activity of a novel family of polymeric surfactants", ***European Polymer Journal***, Vol. 38, No. 7, (2002), 1457-1463.
26. Karlberg, M., Thuresson, K. and Lindman, B., "Hydrophobically modified ethyl (hydroxyethyl) cellulose as stabilizer and emulsifying agent in macroemulsions", ***Colloids and Surfaces A: Physicochemical and Engineering Aspects***, Vol. 262, No. 1, (2005), 158-167.
27. Chronakis, I.S., Egermayer, M. and Piculell, L., "Thermoreversible gels of hydrophobically modified hydroxyethyl cellulose cross-linked by amylose", ***Macromolecules***, Vol. 35, No. 10, (2002), 4113-4122.
28. Zhou, Q., Malm, E., Nilsson, H., Larsson, P.T., Iversen, T., Berglund, L.A. and Bulone, V., "Nanostructured biocomposites based on bacterial cellulosic nanofibers compartmentalized by a soft hydroxyethyl cellulose matrix coating", ***Soft Matter***, Vol. 5, No. 21, (2009), 4124-4130.
29. Aldissi, M. and Armes, S., "Colloidal dispersions of conducting polymers", ***Progress in Organic Coatings***, Vol. 19, No. 1, (1991), 21-58.
30. Eisazadeh, H., Spinks, G. and Wallace, G., "Electrochemical properties of conductive electroactive polymeric colloids", in ***Materials forum, Institute of Metals and Materials Australasia.*** Vol. 16, (1992), 341-344.
31. Aldissi, M., "Is there a colloid in every solution-processable conducting polymer?", ***Advanced Materials***, Vol. 5, No. 1, (1993), 60-62.
32. Eisazadeh, H., Wallace, G. and Spinks, G., "Influence of steric stabilizers on the electropolymerization and properties of polypyrroles", ***Polymer***, Vol. 35, No. 8, (1994), 1754-1758.
33. Chattopadhyay, D., Chakraborty, M. and Mandal, B.M., "Dispersion polymerization of aniline using hydroxypropylcellulose as stabilizer: Role of rate of polymerization", ***Polymer International***, Vol. 50, No. 5, (2001), 538-544.
34. Yang, X. and Lu, Y., "Preparation of polypyrrole-coated silver nanoparticles by one-step uv-induced polymerization", ***Materials Letters***, Vol. 59, No. 19, (2005), 2484-2487.
35. Zhang, H., Li, G., An, L., Yan, T., Gao, X. and Zhu, H., "Electrochemical lithium storage of titanate and titania nanotubes and nanorods", ***The Journal of Physical Chemistry C***, Vol. 111, No. 16, (2007), 6143-6148.

Characterization of Polypyrrole Hydroxyethyl Cellulose/TiO_2 Nanocomposite: Thermal Properties and AFM Analysis

M. Tanzifi[a], Z. Taghipour Kolaei[b], M. Kolbadi nezhad[c], M. Roushani[d]

[a]*Department of Chemical Engineering, Faculty of Engineering, University of Ilam, Ilam, Iran*
[b]*Department of Chemical Engineering, Faculty of Engineering, Babol University of Technology, Babol, Iran*
[c]*School of Chemical Gas and Petroleum Engineering, Semnan University, Semnan, Iran*
[d]*Department of Chemistry, University of Ilam, Ilam, Iran*

P A P E R I N F O

Paper history:
Received 12 September 2014
Received in revised form 12 December 2014
Accepted 18 December 2014

Keywords:
Polypyrrole
Hydroxyethyl cellulose
TitaniumDioxide
Thermal Properties
AFM Analysis

چکید

نانوکامپوزیت پلی پیرول-هیدروکسی اتیل سلولز/ دی اکسید تیتانیوم بوسیله روش پلیمریزاسیون اکسایشی شیمیایی در دمای اتاق و در محلول آب و آب/اتیل استات در حضور فریک کلراید سنتز شد. تاثیر نانوذرات دی اکسید تیتانیوم و هیدروکسی اتیل سلولز روی خواص محصولات از قبیل پایداری حرارتی و مورفولوژی بررسی شد. مورفولوژی و ساختار کامپوزیت و نانوکامپوزیت ساخته شده، بوسیله میکروسکوپ نیروی اتمی (AFM)، میکروسکوپ الکترونی پویشی (SEM)، طیف سنج تبدیل فوریه مادون قرمز (FTIR)، پراش اشعه ایکس (XRD) و آنالیز توزیع حرارتی (TGA) مورد بررسی قرار گرفت. تصاویر AFM محصولات نشان داد که هیدروکسی اتیل سلولز سختی سطح نانوکامپوزیت را کاهش داد. همچنین هیدروکسی اتیل سلولز سایز ذرات را کاهش داد. ساختار مولکولی محصولات بوسیله طیف سنج FTIR تعیین شد. نتایج XRD، ساختار کریستالی نانوذرات TiO_2 و ساختار نسبتا کریستالی نانوکامپوزیت PPY-HEC/TiO_2 را تائید کرد. آنالیز توزیع حرارتی (TGA)، به منظور مطالعه رفتار حرارتی نانوکامپوزیت استفاده شد. نمودارهای TGA نشان داد که HEC و TiO_2 پایداری حرارتی محصولات را افزایش دادند.

***doi**: 10.5829/idosi.ije.2015.28.05b.02*